JOURNAL OF MATERIALS SCIENCE 31 (1996) 5327–5332

Sintering of fibrous barium titanate powder compacts with preferred orientation

YOSHINOBU OHARA, TAKESHI TAKI
Ceramics Research Department, Central Research Laboratory, Sekisui Plastic Co. Ltd, Morimoto 670, Tenri-city, Nara, Japan 632

MASARU MIYAYAMA
Research Center for Advanced Science and Technology, The University of Tokyo, 4-6-1 Komaba, Megro-ku, Tokyo, Japan 153

HIROAKI YANAGIDA
Department of Industrial Chemistry, Faculty of Engineering, The University of Tokyo, Hongo, Bunkyo-ku, Tokyo, Japan 113

The sintering of fibrous $BaTiO_3$ powder particles was investigated. Special emphasis was given to the role of particle orientation in the compact on densification and microstructure development. Compacts were made by dry-pressing. During the initial stage of sintering, the fibrous particles rearranged and bundles of particles were formed. The volume of pores between bundles of particles decreased on further heating. Grain growth started when the sintered density reached ca. 56% of the theoretical density. Higher temperatures of sintering increased the degree of the crystal axis orientation. Thus, highly orientated sintered bodies with high densities were prepared by heating at 1500 °C.

1. Introduction

Grain-oriented ceramics can be prepared by sintering green compacts consisting of plate- or needle-like powder particles which are aligned by the doctor-blade process (tape-casting) [1]. The mechanism of particle orientation during tape-casting and the sintering behaviour of anisotropic powder particles must be understood in order to obtain dense, highly-orientated ceramics [2,3]. On the other hand, grain-oriented ceramics can also be prepared by sintering green compacts containing plate-like powder particles which are aligned by a two-step pressing process [4].

In our previous paper [5], the effect of processing parameters on the orientation of fibrous $BaTiO_3$ particles in a green compact was examined, and the mechanism of particle alignment was discussed. The $BaTiO_3$ fibres dealt with in the paper were 50–100 μm in length.

The present paper focuses on the effect of particle orientation in green compacts on the sintering of "fibrous" powders. Only a few works have discussed the role of powder morphology on sintering [6–9]. Since the degree of orientation in the green compact changes with fibrous powder shape (for example, the length of the fibre), in the present study, fibrous $BaTiO_3$ powder made from potassium titanate, having a longer length than that used in the previous study [5], was used to make compacts with a high degree of orientation.

In this study, the sintering behaviour, such as densification and final grain orientation, was examined for dry-pressed compacts with two-dimensional orientation of fibrous particles. Although $BaTiO_3$ has only average dielectric and piezoelectric properties, it was chosen as a model material because of its simple chemical composition.

2. Experimental procedure

2.1. Synthesis of fibrous $BaTiO_3$

A mixture of potassium titanate long fibres, $2K_2O{\cdot}11TiO_2{\cdot}3H_2O$ (B-type, XI-phase; 100–500 μm long and 10–50 μm in diameter, Kyushu refractories Co. Ltd., Okayama, Japan) and $Ba(OH)_2{\cdot}8H_2O$ (Wako, Oh-saka, Japan) were placed (20 : 61.8 weight ratio) in a silver crucible with water, hydrothermally treated in an autoclave at 150 °C for 24 h under a pressure of 3.5 kg cm^{-2}, and cooled at 5 °C min^{-1}. The products were filtered, washed with water and dried at 80 °C for 24 h. Long fibrous $BaTiO_3$ powders (hereafter called B-type $BaTiO_3$) were obtained.

2.2. Sintering of B-type $BaTiO_3$

Compacts were made by dry-pressing the powder uniaxially under a pressure of 100 MPa for 1 min into a disc 12.5 mm in diameter and ca. 1 mm thick. The sintering behaviour in air was followed by examining changes in density and by observation of the microstructure for compacts heated in air. Samples were placed in a furnace heated at constant temperature and removed after the desired heating time. The

0022–2461

density was determined from the sample dimensions and weight, and was represented by a percentage of the theoretical density (6.02 g cm^{-3}) calculated from the lattice parameters [10].

2.3. Evaluation

The degree of orientation with respect to the crystal axis was determined by X-ray diffraction (XRD) analysis using CuK_α radiation (RAD-2C, Rigku Co. Ltd., Tokyo, Japan). The *c*-axis in the tetragonal form of $BaTiO_3$ lies perpendicular to the length of the fibres and the *a*-axis lies along the length of the fibres. Using Lotgering's method [11], the degrees of *a*- and *c*-axes orientation, *f* (%), were calculated using

$$f = (P - P_0)/(1 - P_0) \quad (1)$$

$$P = \sum(I_{h\,0\,0} + I_{0\,0\,l})/\sum I_{\text{total}} \quad (2)$$

where $\sum(I_{h\,0\,0} + I_{0\,0\,l})$ represents the integrated intensities for $(h\,0\,0)$ and $(0\,0\,l)$, and $\sum I_{\text{total}}$ represents the total integrated intensity for $(h\,k\,l)$ reflections between $2\theta = 20$ and 70°. P_0 is a value of P for a randomly oriented powder. The degree of orientation of green compacts and sintered compacts was measured at the surfaces.

The microstructures were observed by scanning electron microscopy (SEM; JSM-T300, Jeol Co. Ltd., Tokyo, Japan) on fibres and natural surfaces of compacts in the pressing directions.

3. Results

Fig. 1 shows the microstructure of B-type $BaTiO_3$ fibres (a) and the green compact (b). Fibres were normally 100–500 μm long, and under the most favourable conditions, 500–1000 μm long (average diameter 50 μm). Ohara *et al.* [5] reported that the fibres (hereafter called A-type $BaTiO_3$) reported were normally 50–100 μm long, and under the most favourable conditions, 200–300 μm long (average diameter 25 μm). This difference may have been due to the size of potassium titanate as starting materials. The characterization of fibres is summarized in Table I. The green compact exhibited orientation of particles at the surfaces. The compacts exhibited particle alignment in the interior of the compact as well as at the surface. The density of the green compact was 3.0 g cm^{-3}.

These green compacts of B-type $BaTiO_3$ fibres were heated to between 1250 and 1500 °C for 1 h. Fig. 2 shows the densification characteristics. The maximum densities were obtained at sintering temperatures of 1450 °C. Increasing the temperature to 1500 °C resulted in a slight decrease in density.

Fig. 3 shows XRD patterns of the planes perpendicular to the pressing direction in compacts sintered at various temperatures. It can be seen that the relative X-ray intensity of (1 0 0) and (2 0 0) planes for the *a*-axis changed with increasing sintering temperature. This result strongly suggests a preferred orientation of the *a*-axis of a cell tetragonal to the pressing direction.

The degrees of orientation in the green compact were estimated to be 6.3%. Fig. 4 shows the degree of orientation at the surfaces of sintered compacts. The degree of orientation at the surface decreased in samples sintered up to 1300 °C, but > 1300°C it increased with an increase in sintering temperature. The degree of orientation of nearly 7% in samples sintered at 1500 °C was mainly due to the peaks of $(h\,0\,0)$.

Fig. 5 shows microstructures of surfaces perpendicular to the pressing direction in compacts sintered between 1250 and 1500 °C for 1 h. For all compacts, surfaces, as well as the interior, had a large degree of orientation, i.e. dry-pressing caused extensive particle alignment at both the surface and in the interior. Fine grains on the surface of fibrous particles decreased after sintering at 1250 °C and bundles were formed. This fibrous particles group is referred to as "a bundle". The number of bundles increased and fine grains with bundles were eliminated after sintering at 1300 °C.

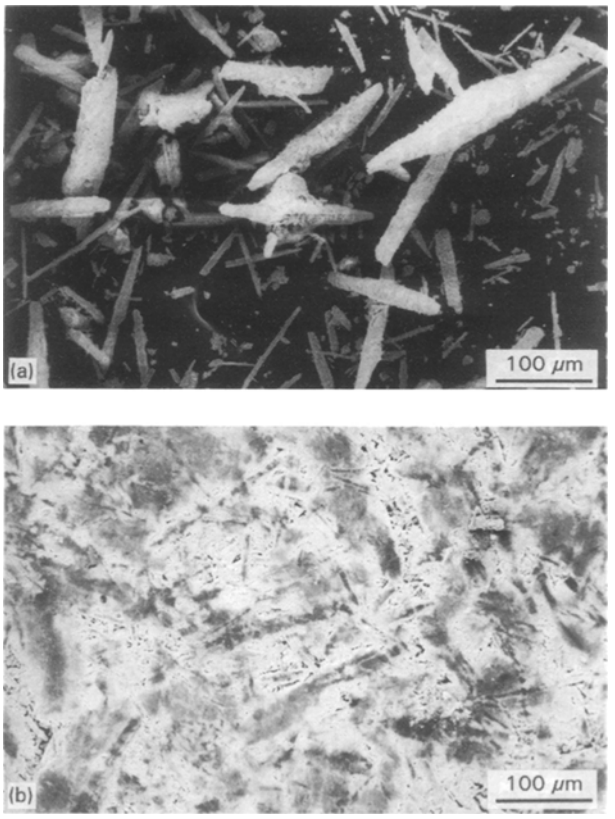

Figure 1 SEM micrographs of the fibre (a) and the surface perpendicular to the pressing direction for the green compact (b) (bar = 100 μm).

TABLE I Characterization of the fibres

	A-type [5]	B-type
Material	$2K_2O \cdot 11TiO_2 \cdot 3H_2O$	
Crystal phase	XI	XI
Fibrous diameter (μm)	1–10	10–100
Fibrous length (μm)	100–500	100–1000
Material	$BaTiO_3$	
Fibrous diameter (μm)	1–5	10–50
Fibrous length (μm)	50–100 (200–300)[a]	100–500 (500–1000)[a]

[a] Fibrous length (μm) under the most favourable conditions.

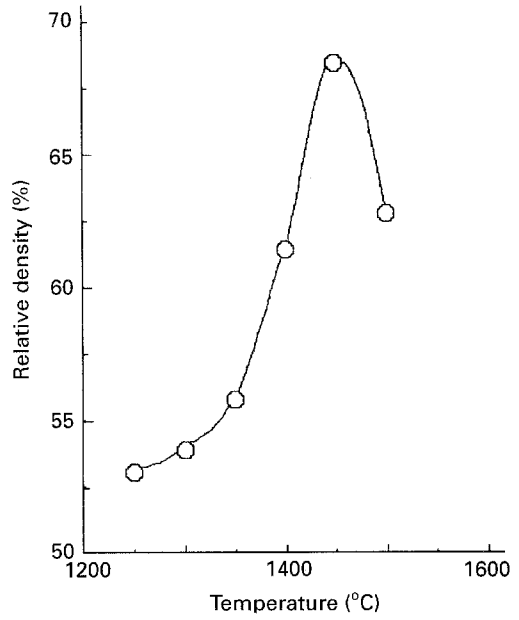

Figure 2 Density of compacts sintered at different temperatures for 1 h.

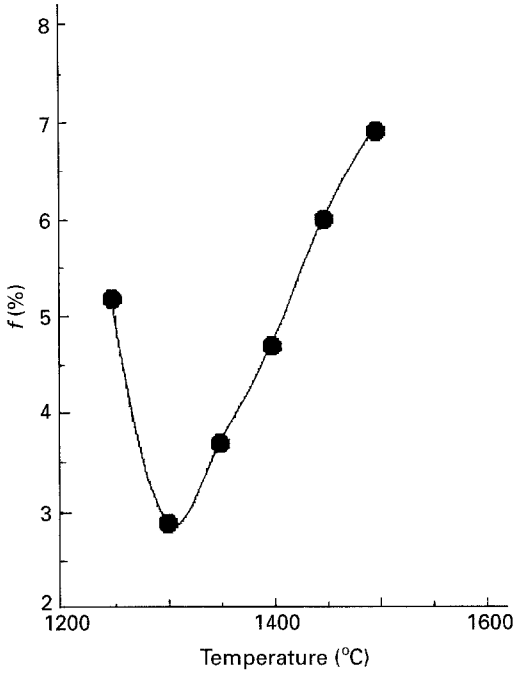

Figure 4 Degree of orientation at the surfaces of compacts sintered for 1 h at given temperatures.

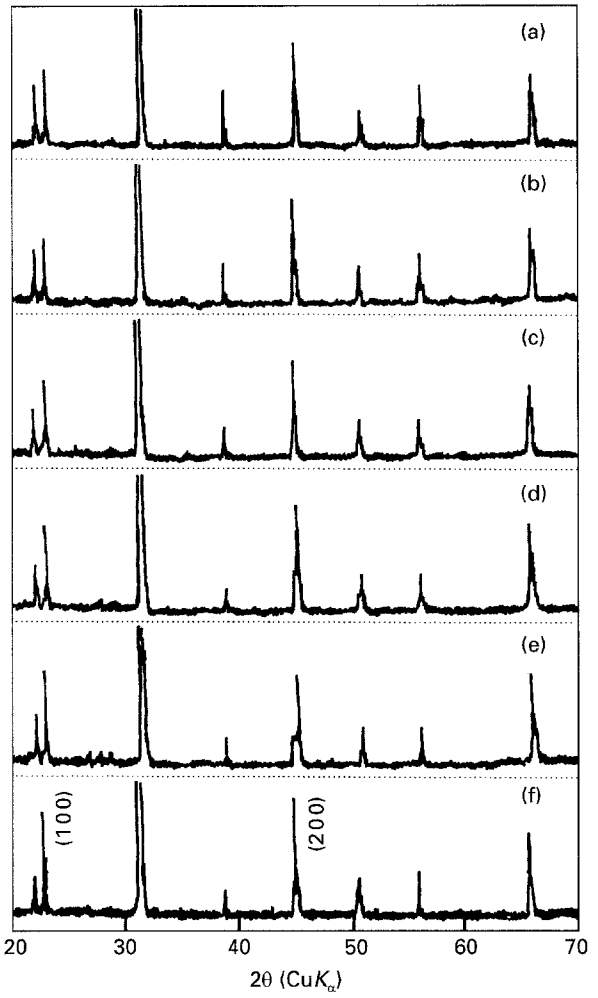

Figure 3 XRD peaks at the surfaces of compacts sintered at 1250 °C (a), 1300 °C (b), 1350 °C (c), 1400 °C (d), 1450 °C (e) and 1500 °C (f) for 1 h.

The fibres in the bundle began to grow on thick fibres like a rectangular pillar at 1350 °C, and the bundle structure started to disappear (Fig. 5c). At the same time, the size of pores between bundles increased with an increase in sintering temperature. Face-to-face contacts between thick fibres developed at 1400 °C and well oriented grains were formed.

Above 1450 °C, well oriented grains grew in a direction parallel to the plate plane on the fibre, resulting in the formation of some elongated grains (Fig. 5e). Extensive grain growth parallel and perpendicular to the plate plane on the fibre was observed at 1500 °C and large pores were formed.

Fig. 6 shows SEM micrographs at high magnifications of Fig. 5. Fine grains on the surface of fibrous particles were found after sintering at 1250 °C and the grains were 1–3 μm in diameter (Fig. 6a). Grain growth began at 1350 °C, as shown in Fig. 6c.

4. Discussion

The sintering behaviour of compacts can be summarized as follows. Bundles were formed during the initial stage of sintering, pores within bundles disappeared first and then the volume of pores between bundles increased. Thick fibrous grains started to grow > 1350 °C and the degree of orientation increased above that temperature.

4.1. Densification

A comparison of the microstructures of the green compact (Fig. 1b) and sintered body heated at 1250 °C for 1 h (Fig. 5a) indicates that bundles are formed by rearrangement of fibrous particles. The rearrangement is assumed to proceed by particle rotation around the fibre axis. A fibrous particle with its plate face nearly parallel to one of the neighbouring particles would rotate and form face-to-face contact with the neighbouring particle. Because fibrous $BaTiO_3$ was in the

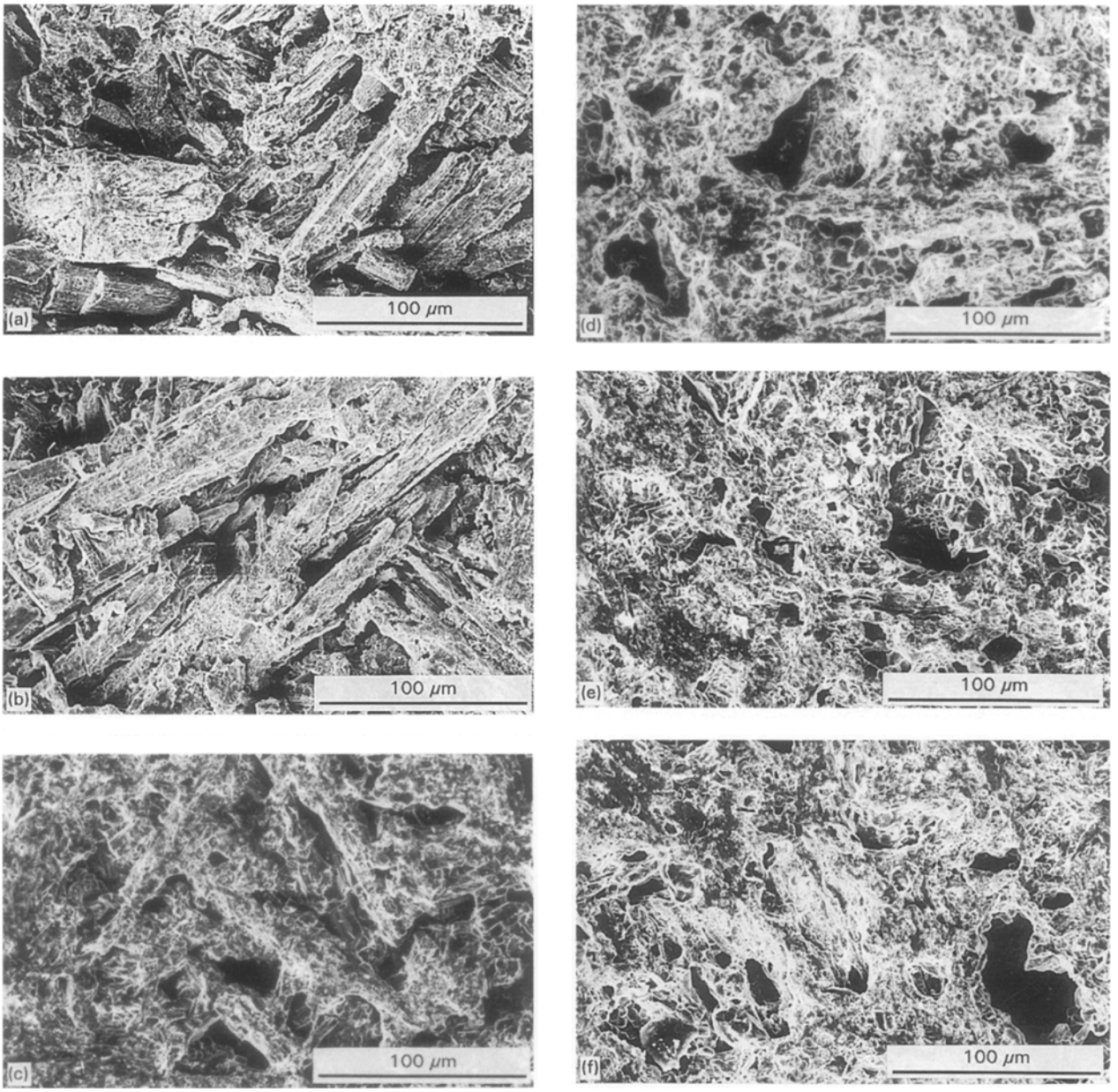

Figure 5 SEM micrographs of the natural surfaces perpendicular to the pressing direction for compacts sintered at 1250 °C (a), 1300 °C (b), 1350 °C (c), 1400 °C (d), 1450 °C (e) and 1500 °C (f) for 1 h (bar = 100 μm).

shape of a square pillar, and has a plate-like surface, several particles with nearly the same orientation seem to form one bundle. The number of particles in one bundle increased as sintering proceeded (cf. Fig. 5a and b).

Pores between particles in the bundle would disappear during the formation of face-to-face contact, and elimination of pores within the bundles would cause either densification or growth of pores between the bundles (pore accumulation).

Petzow and Exner [12] proposed asymmetric neck formation as the origin of particle rotation during solid-state sintering. In the present case, an asymmetric neck would occur because of the deviation from sphericity and anisotropy of surface energy. The presence of wedge-like pores indicates that the grain boundary energy between faces is low, resulting in the formation of face-to-face contact by particle rotation [13].

Because of a large degree of orientation in green compacts, and formation of bundles at low temperatures, densification starts at a higher temperature than in the random compact. Rearrangements of particles and bundle formation are assumed to be the main mechanisms for densification. The smaller the misorientation between particles and bundles, the larger the driving forces for the particle and bundle rearrangements, respectively. The magnitude of rotation of particles and bundles is also dependent on the degree of orientation.

4.2. Orientation

The density of the sintered compact decreased at 1500 °C. At this temperature, rapid heating seems to cause extensive grain growth (Fig. 5e and f). Under these circumstances, pore growth results from pore coalescence [14]. Extensive grain growth seems to be

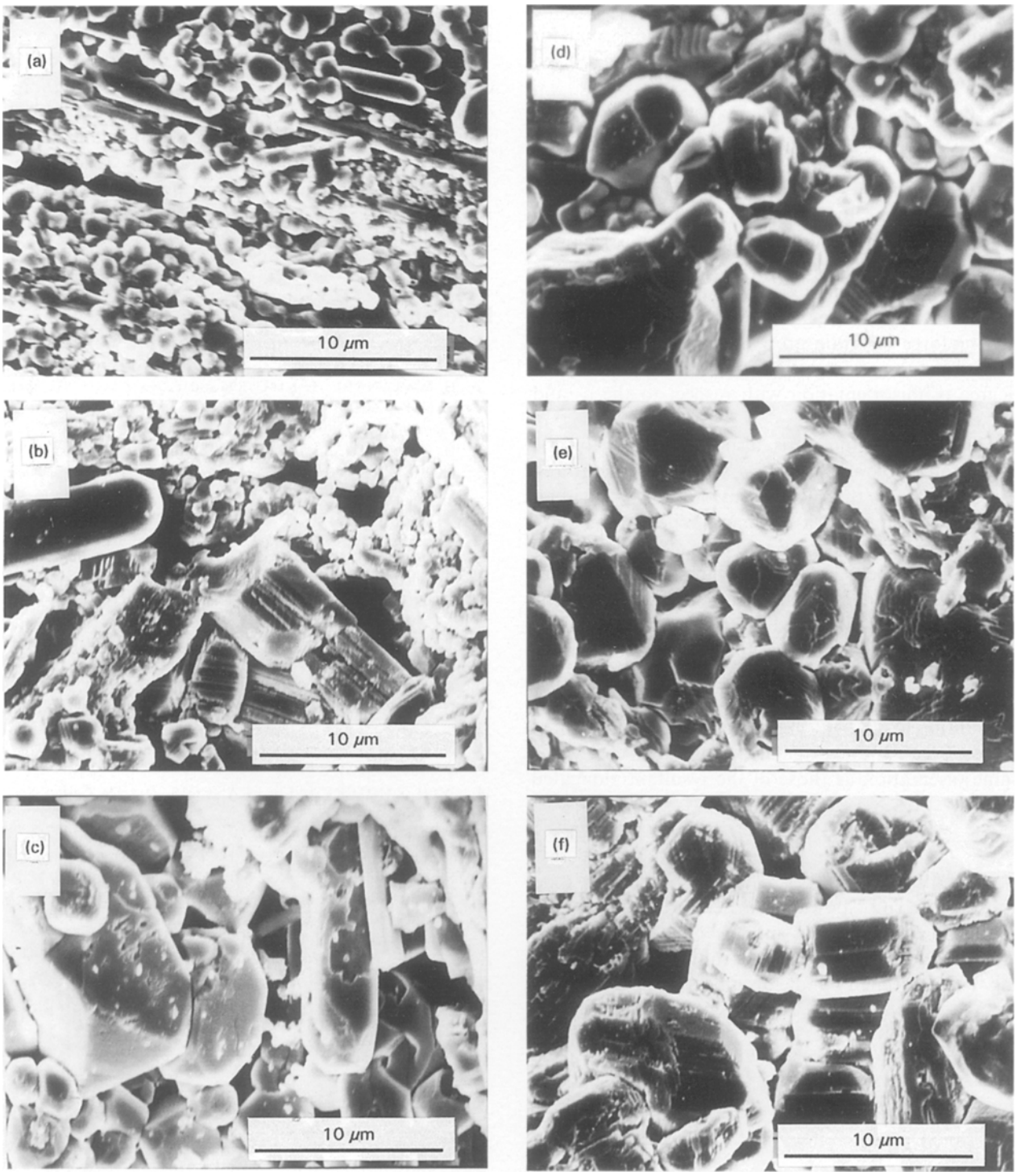

Figure 6 SEM micrographs of the microstructure for compacts sintered at 1250 °C (a), 1300 °C (b), 1350 °C (c), 1400 °C (d), 1450 °C (e) and 1500 °C (f) for 1 h (bar = 10 μm).

responsible for the decreased sintered density. Although this argument is based on equaxed pores, it might be applicable for pores with an anisotropic shape [15].

The degree of orientation decreased until bundle formation occurred (up to 1300 °C). Bundle formation might distribute the direction of the axes in particles, so that the change in the degree of orientation was negative. Although all grains have an equal chance to undergo grain growth, the large population of oriented grains is likely to increase the chance of earlier grain growth. Growing grains consumes neighbouring misoriented smaller grains belonging to the adjacent bundle, and increases their diameter and thickness. Thus, the bundle structure disappears (Fig. 5c).

The grain growth behaviour of $BaTiO_3$ is known to be different from that of normally isotropic materials. The driving force of grain boundary migration is proportional to grain boundary energy and curvature [16]. In ordinary isotropic materials, the grain boundary energy is assumed to be isotropic. In the present case, however, grain boundary energy between grains with face-to-face contact is small. The curvature is assumed to be inversely proportional to grain size for isotropic materials, but the boundary between the

grains with face-to-face contact is nearly flat. Thus, the driving force for grain boundary migration is small for the direction perpendicular to the plate plane on the fibre.

From this point of view, the aspect ratio should decrease during grain growth. This is observed $> 1400\,^{\circ}C$ (Figs 5d and 6d). A different mechanism operates in this case. If two grains come into contact at the plate plane, the *a*-axis of the grains is completely parallel, but the orientation of the *c*-axis is random. When the misorientation with respect to the *c*-axis is small, the grain boundary will disappear by small movement of the atoms in the lattice. In this case, the driving force for grain growth is the grain boundary energy, but the grain growth rate is determined by the degree of misorientation with respect to the *a*- and *c*-axes.

The grain alignment is also responsible for the formation of elongated grains at high temperatures. Fig. 5e indicates that well oriented grains grew in an elongated manner in a compact. When grains with a similar orientation come into contact at their edges, the boundary between grains, which is perpendicular to the plate plane, has large mobility, leading to the formation of an elongated grain. The probability of formation of this kind of grain boundary is proportional to the degree of orientation in the compact after bundle rearrangement. The increase in the degree of orientation is small during the formation of elongated grains because the original grains have nearly the same orientation as those of the resultant elongated grain.

5. Conclusions

Fibrous $BaTiO_3$ powder particles rearranged and formed particle bundles in which particles were in face-to-face contact during the initial stage of sintering. Pores within a bundle disappeared during bundle formation, and those between bundles shrank during bundle rearrangement.

Particle orientation in the green compacts made by dry-pressing influenced the sintering temperature. The degree of orientation decreases during bundle formation but increases during bundle rearrangement and grain growth. When the sintered density reached ca. 56% of the theoretical value, grain growth started, resulting in a significant increase in the degree of orientation.

References

1. M. GRANAHAN, M. HOLMES, W. A. SHULZE and R. E. NEWNHAM, *J. Amer. Ceram. Soc.* **64** (1981) C-68.
2. H. WATANABE, T. KIMURA and T. YAMAGUCHI, *ibid.* **72** (1989) 289.
3. *Idem., ibid.* **74** (1991) 139.
4. H. IGARASHI, *Electronic Ceram.* **Winter** (1981) 57.
5. Y. OHARA, K. KOUMOTO and H. YANAGIDA, *J. Amer. Ceram. Soc.* **68** (1985) C-108.
6. M. YOKOTA, K. KANBARA and J. IMAZU, *Funtai oyobi Funmatsu Yakin* **37** (1990) 127.
7. Y. INOUE, T. KIMURA and T. YAMAGUCHI, *Bull. Amer. Ceram. Soc.* **62** (1983) 704, 711.
8. H. CHAZONE, T. KIMURA and T. YAMAGUCHI, *Yogyo Kyokaishi* **94** (1986) 324.
9. T. YAMAGUCHI and H. KOSHA, *J. Amer. Ceram. Soc.* **66** (1983) 210.
10. R. BECHMAN, *J. Acoust. Soc. Amer.* **28** (1956) 347.
11. F. K. LOTGERING, *J. Inorg. Nucl. Chem.* **9** (1959) 113.
12. G. PETZOW and H. E. EXNER, *Z. Metallkd.* **67** (1976) 611.
13. G. HERRMANN, H. GLEITER and G. BARO, *Acta Metall.* **2** (1989) 353.
14. W. D. KINGERY and B. FRANCOIS, *J. Amer. Ceram. Soc.* **48** (1965) 546.
15. F. A. NICHOLS, *J. Appl. Phys.* **37** (1966) 4599.
16. J. E. BURKE and J. H. ROSOLOWSKI, in "Treaties on Solid State Chemistry, Vol. 4, Reactivity of Solids", edited by N. B. Hannay (Elsevier Seguoia. S.A., Switzerland, 1976) p. 621.

Received 29 September 1994
and accepted 13 February 1996